

# **Discrete Ricci Flow applied to Complex Networks**

**Ollivier-Ricci Curvature and Its Relevance to Community Detection**

**Lorenzo Fabbri  
Giancarlo Oancia**

This essay is submitted for the exam of  
*Complex Networks*



Department of Physics  
Theoretical Physics Curriculum  
University of Bologna  
01/03/2025



## ABSTRACT

---

This project uses Ricci Flow as a geometric approach to detect community structures in networks. It applies Ollivier-Ricci curvature to adjust the weights of edges in a graph, iterating the process to shrink intra-community edges and stretch inter-community edges. Having tested the Ricci Flow method, our goal was identifying the pre-labelled communities of a real dataset: Zachary's Karate Club graph [15].



# CONTENTS

---

<b>1</b>	<b>Overview of the Project</b>	<b>1</b>
<b>2</b>	<b>Introduction and Motivation</b>	<b>3</b>
2.1	Poincaré Conjecture . . . . .	3
2.2	Basics of Differential Geometry . . . . .	6
2.2.1	Differentiable Manifolds . . . . .	7
2.2.2	Differentiable Maps . . . . .	8
2.2.3	Vectors . . . . .	10
2.2.4	One-Forms . . . . .	12
2.2.5	Tensors and Tensor Fields . . . . .	13
2.2.6	Flow generated by a vector field . . . . .	14
2.2.7	Riemannian Manifolds . . . . .	15
2.2.8	Curvature and Ricci tensor . . . . .	17
2.2.9	Covariant Derivative . . . . .	17
2.3	Non-Linear Sigma Models and String Theory . . . . .	17
2.4	Ricci Flow to Tackle Topological Problems . . . . .	19
<b>3</b>	<b>Ricci Flow and Oliver-Ricci Curvature</b>	<b>21</b>
3.1	Riemannian Geometry and Curvature Notions . . . . .	21
3.1.1	Hamilton's Ricci Flow Equation . . . . .	22
3.1.2	From Smooth Settings to Discrete Geometry . . . . .	22
3.2	Optimal Transport and Ollivier's Ricci Curvature . . . . .	23
<b>4</b>	<b>Application to Complex Networks</b>	<b>25</b>
4.1	ARI, Modularity, and Performance . . . . .	26
4.1.1	Adjusted Rand Index (ARI) . . . . .	27

4.1.2	Modularity . . . . .	28
4.1.3	Interpreting Network “Surgery” in This Context . . . . .	30
4.1.4	Algorithmic Complexity and Practical Considerations . . . . .	30
4.1.5	Broader Theoretical Context and Future Directions . . . . .	31
<b>5</b>	<b>The Developed Code</b>	<b>33</b>
5.1	The setup . . . . .	34
5.2	Tests on Synthetic Graphs . . . . .	34
5.2.1	Stochastic Block Model Test Graph . . . . .	34
5.2.2	Lancichinetti-Fortunato-Radicchi Test Graph . . . . .	36
5.2.3	Further Tests on Lancichinetti-Fortunato-Radicchi Graphs . . . . .	38
5.3	Application to Zachary’s Karate Club Graph . . . . .	41
<b>6</b>	<b>Conclusions and Future Directions</b>	<b>45</b>
<b>Appendix A Metric of a 2-sphere</b>		<b>47</b>
<b>References</b>		<b>49</b>

# CHAPTER 1

## OVERVIEW OF THE PROJECT

---

The study of networks has gained considerable attention in various fields, ranging from sociology to biology, and beyond. One of the central problems in network science is community detection, where the objective is to identify groups of nodes (communities) that are more densely connected internally than with the rest of the network. Traditional methods for community detection often rely on statistical or combinatorial approaches. However, recent developments in geometric methods have introduced new ways to approach this problem by leveraging concepts from differential geometry [8].

A powerful geometric tool, the Ricci Flow, originally developed in the context of smooth Riemannian manifolds, can be adapted to discrete network structures. In its original formulation, the Ricci Flow evolves the metric of a manifold according to the curvature (represented by Ricci tensor), leading to a smoothing process over time. Ollivier-Ricci curvature, a discretization of Ricci curvature for graphs, provides a framework to extend this idea to networks, where the "curvature" of edges encodes structural information about node connectivity. Specifically, positive curvature tends to shrink intra-community edges, while negative curvature expands inter-community edges [8].

In this project, we apply Ollivier-Ricci curvature and Ricci Flow to detect the two known communities in Zachary's Karate Club graph. The approach follows the work of Ni et al. [8], where Ricci Flow is used to reshape edge weights iteratively, enhancing the separation between different communities. After applying Ricci Flow, we perform edge surgery to remove weakly connected edges and extract communities as the connected components of the resulting graph.

## **2 | Overview of the Project**

---

The results will be compared to the predefined community labels, allowing for a direct comparison between the detected communities and the actual community structures.

The developed code can be accessed in the corresponding GitHub repository: [\*RicciFlowNetwork\*](#). Code documentation is accessible at [\*CodeDocumentation\*](#).

Diciamo che la prima parte del report è introduttiva e riguarda le stringhe ecc.?

# CHAPTER 2

## INTRODUCTION AND MOTIVATION

---

### 2.1 Poincaré Conjecture

To understand the origins of Ricci Flow and its relevance in the mathematical context, one has to get an insight on its application on geometrical and topological problems. Therefore, to begin with the discussion, we'll introduce the Poincaré conjecture and Perelman's proof.

In the 1985 paper *Analysis Situs* [9], Poincaré laid the foundations for what we call today as *topology*. Its purpose is clearly underlined in the articles, through:

*...geometry is the art of reasoning well from badly drawn figures; however, these figures, if they are not to deceive us, must satisfy certain conditions; the proportions may be grossly altered, but the relative positions of the different parts must not be upset.*

Since there's no reason to follow the historical development, we'll furnish the modern definitions and intuition about topology.

**Definition 1** (Topological space). Let  $X$  be a non-empty set. A *topology* on  $X$  is a family  $\mathcal{A}$  of subsets  $\mathcal{A} \ni A \subseteq X$ , called *open sets*, such that

- The empty set and  $X$  are open sets,

$$\emptyset \in \mathcal{A}, \quad X \in \mathcal{A}. \tag{2.1}$$

- The union of any collection of open sets is again an open set,

$$A_i \in \mathcal{A}, i \in J \implies \bigcup_{i \in J} A_i \in \mathcal{A}, \tag{2.2}$$

with  $J$  a set of indices.

- The intersection of any finite number of open sets is again an open set,

$$A_i \in \mathcal{A}, i = 1, 2, \dots, N \implies \bigcap_{i=1}^N A_i \in \mathcal{A}. \quad (2.3)$$

The set  $X$ , with the topology  $\mathcal{A}$ , is called *topological space*  $(X, \mathcal{A})$ .

We can then define straightforwardly what a closed set is. Notice that we could have defined the topology with closed sets as well.

**Definition 2** (Closed sets). Given  $A \in \mathcal{A}$ , a subset  $C \subseteq X$  is *closed* if it is of the form

$$C \text{ closed} \iff X \setminus C \text{ open.} \quad (2.4)$$

There are some crucial properties of topological spaces which will be extensively used throughout this work. The first, concerns compactness, which is a subtle concept to identify finiteness in this context.

**Definition 3** (Compact). A topological space  $(X, \mathcal{A})$  is called *compact* if every open cover,

$$X \in \bigcup_{\alpha \in C} U_\alpha, \quad (2.5)$$

contains a finite subcover,

$$X \in \bigcup_{i=1}^N U_i. \quad (2.6)$$

Further, another characterizing property of some topological spaces is the connectedness. The intuition is that a connected space can't be cut up into parts that have nothing to do with each other. To make this sentence more precise, we need first to define a path on a topological space.

**Definition 4** (Path). Given a topological space  $(X, \mathcal{A})$  and two points  $x, y \in X$ , a *path* is a continuous function  $f : [0, 1] \rightarrow X$  such that  $f(0) = x$  and  $f(1) = y$ . A *path-component* of  $X$  is an equivalence class of  $X$  under the equivalence relations which makes  $x$  equivalent to  $y$  if and only if there is a path from  $x$  to  $y$ .

**Definition 5** (Connected). A topological space  $(X, \mathcal{A})$  is said to be *connected* if it can't be represented as the union of two or more disjoint non-empty open subsets.

**Definition 6** (Path connected). A topological space  $(X, \mathcal{A})$  is said to be *path connected* if there is exactly one path-component. For non-empty spaces, this is equivalent to the statement that there is a path joining any two points in  $X$ .

**Definition 7** (Simply connected). A topological space  $(X, \mathcal{A})$  is said to be *simply connected* if it is path connected and every path between two points can be continuously transformed into any other such path while preserving the two endpoints in question.

Other than these properties, we need maps from a topological space to another, both for relating these abstract concepts to the Euclidean space, for which we have intuition, and for studying the algebraic properties of the structures. This gives rise to the necessity of defining a homeomorphism.

**Definition 8** (Homeomorphism). A *homeomorphism*, also known as *topological isomorphism*, is a bijective and continuous between topological spaces that has a continuous inverse function.

We should have defined what a continuous map is, but the definition is not too different from the one used in multivariate calculus.

In particular, we're interested in applying those properties to some particular types of topological spaces, that is, topological manifolds. To apply the Ricci Flow to a topological context, the manifold must be further equipped with a wider structure, i.e., must be a Riemannian Manifold. While this topic will be covered in the next section, for now let's just define a Manifold.

**Definition 9** (Manifold). A *topological manifold* is a topological space which locally resembles the real  $n$ -dimensional Euclidean space.

Without delving into the details of the Manifolds with boundaries, we make use of our intuition to understand this concept, and directly define a closed manifold.

**Definition 10** (Closed manifold). A *closed manifold* is a manifold without boundary that is also compact.

A simple example is provided by the circle, for one-dimensional manifolds, and the sphere for two-dimensional ones. We're interested in the 3-sphere, which is a straightforward generalization of the previous examples.

**Definition 11** (3-sphere). In coordinates<sup>1</sup>, a 3-sphere with center  $(C_0, C_1, C_2, C_3)$  and radius  $r$  is the set of all points  $(x_0, x_1, x_2, x_3)$  in  $\mathbb{R}^4$  such that

$$\sum_{i=0}^3 (x_i - C_i)^2 = (x_0 - C_0)^2 + (x_1 - C_1)^2 + (x_2 - C_2)^2 + (x_3 - C_3)^2 = r^2. \quad (2.7)$$

---

<sup>1</sup>We'll define a chart on a manifold later on, for now let's use our intuitive understanding of a set of coordinates in  $\mathbb{R}^n$ .

In particular, the 3-sphere centred at the origin with radius 1 is called the *unit 3-sphere* and is usually denoted as  $S^3$

$$S^3 = \{(x_0, x_1, x_2, x_3) \in \mathbb{R}^4 : x_0^2 + x_1^2 + x_2^2 + x_3^2 = 1\}. \quad (2.8)$$

As a Manifold, the 3-sphere is a compact, connected, 3-dimensional Manifold without boundary. We're now able to understand the formulation of the Poincaré conjecture in its work:

*A simply-connected closed manifold is homeomorphic to a sphere.*

To be fair, at the beginning it didn't think of it as a conjecture, since it considered it a trivial statement. It turned out to be one of the biggest unresolved problems in mathematics. After some refinements during the following years [cite](#), he came up to the final form of its conjecture [10]:

*Every three-dimensional topological manifold which is closed, connected, and has trivial fundamental group is homeomorphic to the three-dimensional sphere.*

To overcome the complexity of fundamental groups and homologies, we'll just quote the following theorem, which allows us to understand the necessity of the presence of the trivial fundamental group in the latter formulation of the conjecture.

**Theorem T.1.** *A path-connected topological space is simply connected if and only if its fundamental group is trivial.*

To understand how to tackle the problem of Poincaré conjecture proof, we first need to investigate the manifold structure of some particular topological spaces.

## 2.2 Basics of Differential Geometry

In order to understand the Ricci Flow applications, it's necessary to study the properties of Riemannian Manifolds, in particular how to define a flow on a Manifold and how this is related to some differential equations. We'll see that the Ricci Flow is nothing but a differential equation for some class of different metrics on a Riemannian Manifold.

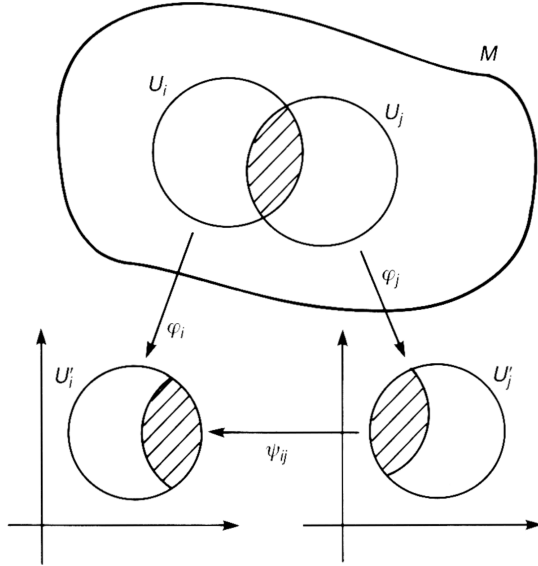


Figure 2.1  $\varphi_i$  is a homeomorphism from  $U_i$  onto an open subset  $U'_i$  of  $\mathbb{R}^n$ .

### 2.2.1 Differentiable Manifolds

Let's first refine the definition of a differentiable Manifold 9.

**Definition 12** (Differentiable manifold).  $\mathcal{M}$  is an  $n$ -dimensional differentiable manifold if

- $\mathcal{M}$  is a topological space.
- $\mathcal{M}$  is provided with a family of pairs  $\{(U_i, \varphi_i)\}$ .
- $\{U_i\}$  is a family of open sets which covers  $\mathcal{M}$ , that is,  $\cup_i U_i = \mathcal{M}$ .  $\varphi_i$  is a homeomorphism from  $U_i$  onto open subsets  $U'_i$  of  $\mathbb{R}^n$ . See fig. 2.1
- Given  $U_i$  and  $U_j$  such that  $U_i \cap U_j \neq \emptyset$ , the map  $\psi_{ij} = \varphi_i \circ \varphi_j^{-1}$  from  $\varphi_j(U_i \cap U_j)$  to  $\varphi_i(U_i \cap U_j)$  is infinitely differentiable.

The pair  $(U_i, \varphi_i)$  is called a *chart*, while the whole family  $\{(U_i, \varphi_i)\}$  is an *atlas*. The subset  $U_i$  is called the *coordinate neighbourhood*, while  $\varphi_i$  is the *coordinate function*. This homeomorphism is represented by  $n$  functions  $\{x_1(p), \dots, x_n(p)\}$ , which are called *coordinates*. However, notice that a point  $p \in \mathcal{M}$  is independent of its coordinates. In each coordinate neighbourhood  $U_i$ ,  $\mathcal{M}$  looks like an open subset of  $\mathbb{R}_n$  whose element is  $\{x^1, \dots, x^n\}$ , and this explains our previous definition 9.

Recall from the previous section that we're interested in Manifolds with boundaries. We're now able to define them.

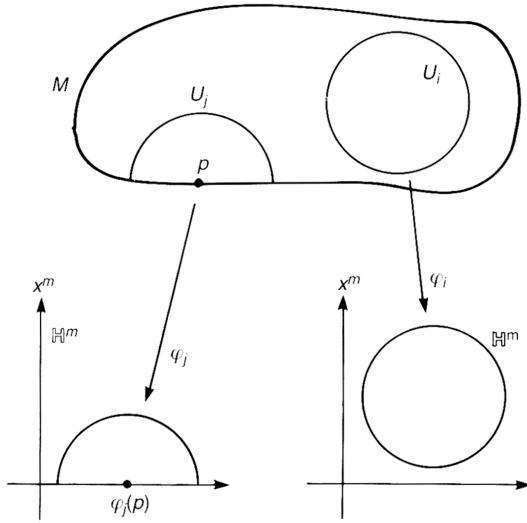


Figure 2.2 A Manifold  $\mathcal{M}$  with boundary. Here,  $p \in \partial\mathcal{M}$ .

**Definition 13** (Manifold with boundary). A *Manifold with boundary* (see fig. 2.2) is a topological space  $\mathcal{M}$  which is covered by a family of open sets  $\{U_i\}$ , each of which is homeomorphic to an open set of  $H^n$ , where

$$H^n := \{(x^1, \dots, x^n) \in R^n | x^n \geq 0\}. \quad (2.9)$$

The set of points which are mapped to points with  $x_n = 0$  is called the *boundary* of  $\mathcal{M}$ , denoted by  $\partial\mathcal{M}$ . The coordinates of  $\partial\mathcal{M}$  may be given by  $n - 1$  numbers  $(x^1, \dots, x^{n-1}, 0)$ . One must then be careful to define smoothness. Indeed, the map  $\psi_{ij}: \varphi_j(U_i \cap U_j) \rightarrow \varphi_i(U_i \cap U_j)$  is defined on an open set of  $H^n$  in general, and  $\varphi_{ij}$  is said to be smooth if it's  $C^\infty$  in an open set of  $\mathbb{R}^n$  which contains  $\varphi_j(U_i \cap U_j)$ .

## 2.2.2 Differentiable Maps

Due to the presence of the differentiable structure on a Manifold, we're able to use the calculus techniques developed for  $\mathbb{R}^n$ . We can define a map between manifolds.

Let  $\mathcal{M}$  and  $\mathcal{N}$  be an  $m$ -dimensional and an  $n$ -dimensional Manifold, respectively. Let's then consider a map between them, i.e.,  $f: \mathcal{M} \rightarrow \mathcal{N}$ , where  $\mathcal{M} \ni p \mapsto f(p) \in \mathcal{N}$ , see fig. 2.3 Taking the charts  $(U, \varphi)$  on  $\mathcal{M}$  and  $(V, \psi)$  on  $\mathcal{N}$ , the coordinate representation of  $f$  will be

$$\varphi \circ f \circ \varphi^{-1}: \mathbb{R}^m \rightarrow \mathbb{R}^n. \quad (2.10)$$

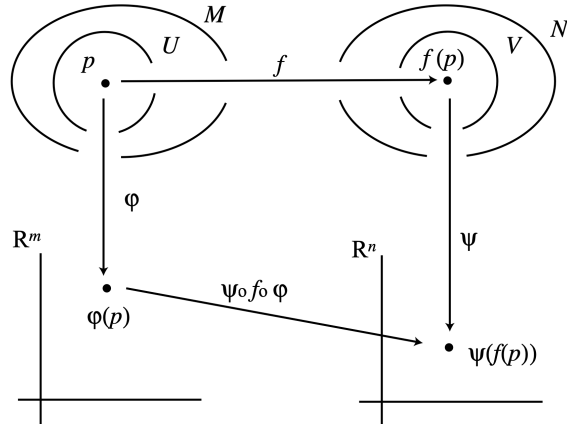


Figure 2.3 A map  $f: \mathcal{M} \rightarrow \mathcal{N}$  has coordinates representation  $\psi \circ f \circ \varphi^{-1}: \mathbb{R}^m \rightarrow \mathbb{R}^n$ .

We can write  $\varphi(p) = \{x^\mu\}$  and  $\psi(f(p)) = \{y^\alpha\}$ , which makes explicit that  $y \equiv \psi \circ f \circ \varphi^{-1}(x)$  is an  $m$ -variables, vector-valued, usual function. Rendering the coordinate charts implicit, we may write  $y^\alpha = f^\alpha(x^\mu)$ , which makes clear why  $f$  is said to be *differentiable* at  $p$  if  $y$  is  $C^\infty$ . Notice, however, that the differentiability of  $f$  is independent of the chosen coordinates.

A very important type of maps between manifold is given by diffeomorphisms.

**Definition 14** (Diffeomorphism). Let  $f: \mathcal{M} \rightarrow \mathcal{N}$  be a homeomorphism and  $\psi$  and  $\varphi$  the same coordinate functions as before. Then, if  $\psi \circ f \circ \varphi^{-1}$  is invertible and both  $y \equiv \psi \circ f \circ \varphi^{-1}(x)$  and  $x \equiv \varphi \circ f^{-1} \circ \psi^{-1}(y)$  are  $C^\infty$ ,  $f$  is called a *diffeomorphism* and  $\mathcal{M}$  is said to be *diffeomorphic* to  $\mathcal{N}$ ,  $\mathcal{M} \equiv \mathcal{N}$ .

Taking a diffeomorphism from a Manifold into itself, we can implement the concept of change of coordinates, in two different interpretation. First, the set of diffeomorphisms  $f: \mathcal{M} \rightarrow \mathcal{M}$  form a group denoted by  $\text{Diff}(\mathcal{M})$ . Considering a particular  $f \in \text{Diff}(\mathcal{M})$ , and a chart  $(U, \varphi)$ , such that, for  $p \in U$  and  $f(p) \in U$ , we get  $\varphi(p) = x^\mu(p)$  and  $\varphi(f(p)) = y^\mu(f(p))$ , then  $y$  is a differentiable function of  $x$  and the above diffeomorphism can be thought as an *active transformation* for a change of coordinates.

However, if  $(U, \varphi)$  and  $(V, \psi)$  are overlapping charts, for a point  $p \in U \cap V$ , there are two coordinates values, i.e.,  $x^\mu = \varphi(p)$  and  $y^\mu = \psi(p)$ . Then, the map  $x \mapsto y$  is differentiable, and it represents a *passive transformation* for a change of coordinates.

Two important kinds of maps are curves and functions.

**Definition 15** (Curve). An *open curve* in an  $n$ -dimensional Manifold  $\mathcal{M}$  is a map  $c: (a, b) \rightarrow \mathcal{M}$ , where  $(a, b)$  is an open interval such that  $a < 0 < b$ . A *closed curve* is

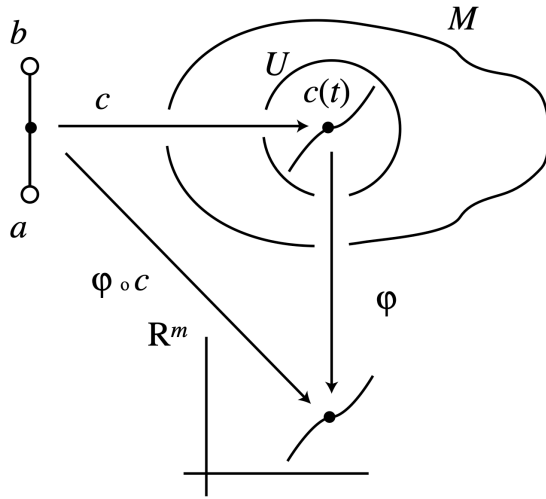


Figure 2.4 A curve  $c$  in  $\mathcal{M}$  and its coordinate representation  $\psi \circ c$ .

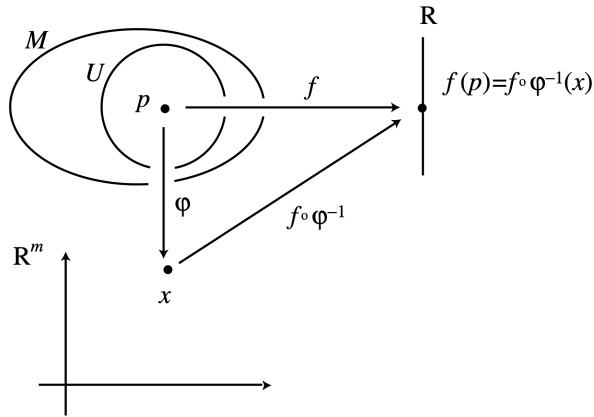


Figure 2.5 A function  $f: \mathcal{M} \rightarrow \mathbb{R}$  and its coordinate representation  $f \circ \varphi^{-1}$ .

a map  $c: S^1 \rightarrow \mathcal{M}$ . On a chart  $(U, \varphi)$ , a curve  $c(t)$  has the coordinate representation  $x = \varphi \circ c: \mathbb{R} \rightarrow \mathbb{R}^n$ . See fig. 2.4

**Definition 16** (Function). A *function*  $f$  on  $\mathcal{M}$  is a smooth map from  $\mathcal{M}$  to  $\mathbb{R}$ . On a chart  $(U, \varphi)$ , the coordinate representation of  $f$  is given by  $f \circ \varphi^{-1}: \mathbb{R}^n \rightarrow \mathbb{R}$ , which is a real-valued function of  $n$  variables. The set of functions is denoted by  $\mathfrak{F}(\mathcal{M})$ . See fig. 2.5

### 2.2.3 Vectors

The curves allow us to define a vector as a differential operator. So understand this more deeply, let's take a Manifold  $\mathcal{M}$ , a curve  $c: (a, b) \rightarrow \mathcal{M}$  and a function  $f: \mathcal{M} \rightarrow \mathbb{R}$ ,

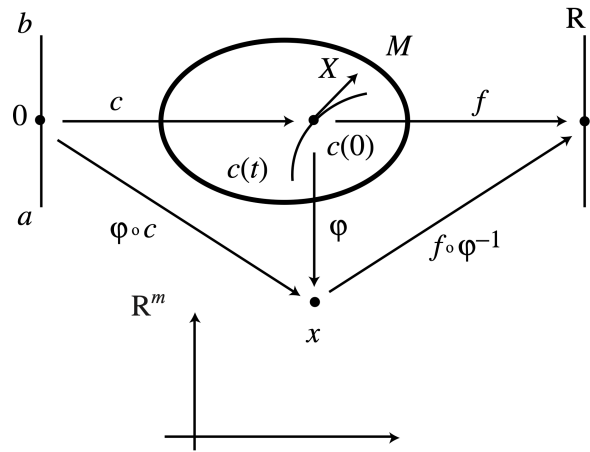


Figure 2.6 A curve  $c$  and a function  $f$  define a tangent vector along the curve in terms of directional derivatives.

where  $(a, b)$  is an open interval containing  $t = 0$ , as showed in fig. 2.6. The tangent vector at  $c(0)$  is defined to be the directional derivative of a function  $f(c(t))$  along the curve  $c(t)$  at  $t = 0$ . In particular,

$$X[f] := \frac{df(c(t))}{dt} \Big|_{t=0} = \frac{\partial f}{\partial x^\mu} \frac{dx^\mu(c(t))}{dt} \Big|_{t=0} = X^\mu \left( \frac{\partial f}{\partial x^\mu} \right), \quad (2.11)$$

where we defined

$$X = X^\mu \left( \frac{\partial}{\partial x^\mu} \right), \quad X^\mu = \frac{dx^\mu(c(t))}{dt} \Big|_{t=0} \quad (2.12)$$

Notice that we used abuse of notation, that is  $\partial f / \partial x^\mu$  really means  $\partial(f \circ \varphi^{-1}(x)) / \partial x^\mu$ .

Trying to be more precise, as known from multivariate analysis, whenever we have a curve, we can define an equivalence class. This case is no different. Indeed, given two curves  $c_1(t)$  and  $c_2(t)$  on  $\mathcal{M}$ , if they satisfy

$$c_1(0) = c_2(0) = p, \quad (2.13a)$$

$$\frac{dx^\mu(c_1(t))}{dt} \Big|_{t=0} = \frac{dx^\mu(c_2(t))}{dt} \Big|_{t=0}, \quad (2.13b)$$

then they yield the same differential operator  $X$  at  $p$ . Then, the above conditions define an equivalence relation  $\sim$  such that  $c_1(t) \sim c_2(t)$ . This allows us to define

**Definition 17** (Vector). A *tangent vector*  $X$  is the *equivalence class of curves*

$$[c(t)] = \left\{ \tilde{c}(t) \mid \tilde{c}(0) = c(0) \wedge \frac{dx^\mu(\tilde{c}(t))}{dt} \Big|_{t=0} = \frac{dx^\mu(c(t))}{dt} \Big|_{t=0} \right\}. \quad (2.14)$$

All the tangent vectors at a particular point  $p \in \mathcal{M}$  form a vector space called *tangent space* of  $\mathcal{M}$  at  $p$ , denoted by  $T_p\mathcal{M}$ . By means of equation (2.12), it's straightforward to see that the basis vectors of this vector space are

$$\left\{ e_\mu = \frac{\partial}{\partial x^\mu} \right\}, \quad \mu = 1, \dots, n. \quad (2.15)$$

Clearly,  $\dim T_p\mathcal{M} = \dim \mathcal{M}$ . Further, for each  $V \in T_p\mathcal{M}$ , we can expand it as  $V = V^\mu e_\mu = V^\mu \partial_\mu$ , and we call  $V^\mu$  the components of  $V$  with respect to the basis.

Obviously,  $\{e_\mu\}$  are not the only possible basis for the vector space  $T_p\mathcal{M}$ . Indeed, as known from linear algebra, an arbitrary linear combination  $\hat{e}_i := A_i^\mu e_\mu$ , with  $A = (A_i^\mu) \in GL(n, \mathbb{R})$ , is a basis as well. In this case,  $\{\hat{e}_i\}$  is called a *non-coordinate basis*.

Further, given that a vector exists independently of its coordinates, we can take two coordinate charts, with a point in the intersection of their domains, i.e.,  $p \in U_i \cap U_j$ , with  $x = \varphi_i(p)$  and  $y = \varphi_j(p)$ . A generic vector  $X \in T_p\mathcal{M}$  can be equivalently expanded as

$$X = X^\mu \frac{\partial}{\partial x^\mu} = \tilde{X}^\mu \frac{\partial}{\partial y^\mu}, \quad (2.16)$$

which shows the relation of the components of a vector in two different charts, i.e,

$$\tilde{X}^\mu = X^\nu \frac{\partial y^\mu}{\partial x^\nu}. \quad (2.17)$$

## 2.2.4 One-Forms

Given that  $T_p\mathcal{M}$  is a vector space, we can define its dual vector space, whose elements are linear functional from  $T_p\mathcal{M}$  to  $\mathbb{R}$ . This space is called *cotangent space*, is denoted by  $T_p^*\mathcal{M}$ , and their elements  $\omega: T_p\mathcal{M} \rightarrow \mathbb{R} \in T_p^*\mathcal{M}$  are called *one-forms*.

The simplest one-form is the *differential* of a function  $f \in \mathfrak{F}(\mathcal{M})$ . Indeed, for a vector  $V \in T_p\mathcal{M}$ , its action on  $f$  is

$$V[f] = V^\mu \frac{\partial f}{\partial x^\mu} \in \mathbb{R}. \quad (2.18)$$

So, we define the action of  $df \in T_p^*\mathcal{M}$  on a vector  $V \in T_p\mathcal{M}$  by

$$\langle df, V \rangle \equiv V[f] = V^\mu \frac{\partial f}{\partial x^\mu} \in \mathbb{R}. \quad (2.19)$$

In coordinates  $x = \varphi(p)$ , the differential can be expanded as

$$df = \frac{\partial f}{\partial x^\mu} dx^\mu, \quad (2.20)$$

which clearly shows that  $\{\mathrm{d}x^\mu\}$  is a basis of  $T_p^*\mathcal{M}$ . In particular, it's the dual basis of  $\{\partial_\mu\}$ , since

$$\langle \mathrm{d}x^\mu, \partial_\mu \rangle = \frac{\partial x^\nu}{\partial x^\mu} = \delta_\mu^\nu. \quad (2.21)$$

It's now easy to consider generic one-forms  $\omega \in T_p^*\mathcal{M}$  and generic vectors  $V \in T_p\mathcal{M}$ . Picking a coordinate basis for the tangent space and its dual basis for the cotangent one, we can expand  $\omega = \omega_\mu \mathrm{d}x^\mu$  and  $V = V^\mu \partial_\mu$ . Then, as usual, we can define an *inner product*  $\langle \cdot, \cdot \rangle : T_p^*\mathcal{M} \times T_p\mathcal{M} \rightarrow \mathbb{R}$  by

$$\langle \omega, V \rangle = \omega_\mu V^\mu \langle \mathrm{d}x^\mu, \partial_\nu \rangle = \omega_\mu V^\nu \delta_\nu^\mu = \omega_\mu V^\mu. \quad (2.22)$$

Finally, analogously than before, we can pick two charts and a point in their domain's intersection,  $p \in U_i \cap U_j$ , so that

$$\omega = \omega_\mu \mathrm{d}x^\mu = \tilde{\omega}_\nu \mathrm{d}y^\nu, \quad (2.23)$$

with  $x = \varphi_i(p)$  and  $y = \varphi_j(p)$ . Then, we can easily infer the transformation rule of a one-form under a change of coordinates, indeed,

$$\mathrm{d}y^\nu = \frac{\partial y^\nu}{\partial x^\mu} \mathrm{d}x^\mu \implies \tilde{\omega}_\nu = \omega_\mu \frac{\partial x^\mu}{\partial y^\nu}. \quad (2.24)$$

## 2.2.5 Tensors and Tensor Fields

From multilinear algebra, it should be familiar that a *tensor* of type  $(p, q)$  is a multilinear map which maps  $q$  elements of  $T_p^*\mathcal{M}$  and  $r$  elements of  $T_p\mathcal{M}$  to a real number:

$$T^{(q,r)} : \underbrace{T_p^*\mathcal{M} \otimes \cdots \otimes T_p^*\mathcal{M}}_{q \text{ times}} \otimes \underbrace{T_p\mathcal{M} \otimes \cdots \otimes T_p\mathcal{M}}_{r \text{ times}} \longrightarrow \mathbb{R}. \quad (2.25)$$

Picking a coordinate basis and its dual basis,

$$T^{(q,r)} = T^{\mu_1 \dots \mu_q}_{\nu_1 \dots \nu_r} \frac{\partial}{\partial x^{\mu_1}} \dots \frac{\partial}{\partial x^{\mu_q}} \mathrm{d}x^{\nu_1} \dots \mathrm{d}x^{\nu_r}. \quad (2.26)$$

The set of type  $(q, r)$  tensors at  $p \in \mathcal{M}$  is denoted by  $\mathcal{T}_{r;p}^q(\mathcal{M})$ . Further, taking  $r$ -vectors  $V_a = V_a^\mu \partial_\mu$  and  $q$  one-forms  $\omega_a = \omega_{a\mu} \mathrm{d}x^\mu$ , the action of  $T^{(q,r)}$  on them is given by

$$T(\omega_1, \dots, \omega_q; V_1, \dots, V_r) = T^{\mu_1 \dots \mu_q}_{\nu_1 \dots \nu_r} \omega_{1\mu_1} \dots \omega_{q\mu_q} V_1^{\nu_1} \dots V_r^{\nu_r}. \quad (2.27)$$

In order to probe a Manifold structure, it's necessary to have fields defined in it, i.e., structures which are smoothly defined for each point of  $\mathcal{M}$ . Knowing the tensor structure at a point, it's easy to generalize it to the entire Manifold. To begin with, let's consider the simplest tensor, i.e., a vector, which is a  $(1, 0)$  tensor.

A *vector field* is a vector assigned smoothly to each point of  $\mathcal{M}$ . In other words,  $V$  is a vector field if  $V[f] \in \mathfrak{F}(\mathcal{M})$ , for any  $f \in \mathfrak{F}(\mathcal{M})$ . Then, each component of a vector field is itself a smooth function from  $\mathcal{M}$  to  $\mathbb{R}$ . We denote the set of vector fields with  $\mathfrak{X}(\mathcal{M})$ . Then, a vector  $X \in \mathfrak{X}(\mathcal{M})$  computed at a point  $p \in \mathcal{M}$  is a vector at  $T_p\mathcal{M}$ , i.e.,  $X|_p \in T_p\mathcal{M}$ .

Similarly, a *tensor field* of type  $(q, r)$  is a smooth assignment of an element of  $\mathcal{T}_{r;p}^q(\mathcal{M})$  at each point  $p \in \mathcal{M}$ . The set of tensor fields of type  $(q, r)$  on  $\mathcal{M}$  is denoted by  $\mathcal{T}_r^q(\mathcal{M})$ .

An important tensor field we're interested in is the metric tensor, which is tightly related to the definition of a Ricci Flow, in the context of Riemannian Manifolds. However, let's first study an important property of vector fields: they can generate a flow on a Manifold. Studying further the relation among flows and differential equation, allows us to better grasp the definition of a Ricci Flow.

### 2.2.6 Flow generated by a vector field

Let  $X$  be a vector field in  $\mathcal{M}$ ,  $X \in \mathfrak{X}(\mathcal{M})$ . An *integral curve*  $x(t)$  of  $X$  is a curve in  $\mathcal{M}$ , whose tangent vector at  $x(t)$  is  $X|_{x(t)}$ . In a chart  $(U, \varphi)$ , this is equivalent to

$$\frac{dx^\mu}{dt} = X^\mu(x(t)), \quad (2.28)$$

where  $x^\mu(t)$  is the  $\mu$ -th component of  $\varphi(x(t))$  and  $X = X^\mu \partial_\mu$ . Pay attention to the abuse of notation. Indeed, we used  $x$  to denote both a point on  $\mathcal{M}$  and its coordinates.

Then, to finding the integral curve of a vector field  $X$  is equivalent to solving the system of ODEs (2.28), with initial condition  $x_0^\mu = x^\mu(0)$ , which are the coordinates of the integral curve at  $t = 0$ .

The existence and uniqueness theorem of ODEs guarantees that there is a unique solution to (2.28), at least locally, with the initial condition  $x_0^\mu$ .

Let, then,  $\sigma(t, x_0)$  be an integral curve of  $X$  passing through a point  $x_0$  at  $t = 0$  and let's denote its coordinates by  $\sigma^\mu(t, x_0)$ . Then, eq. (2.28) becomes

$$\frac{d}{dt} \sigma^\mu(t, x_0) = X^\mu(\sigma(t, x_0)), \quad (2.29)$$

with the initial condition

$$\sigma^\mu(0, x_0) = x_0^\mu. \quad (2.30)$$

The map  $\sigma: \mathbb{R} \times \mathcal{M} \rightarrow \mathcal{M}$  is called *flow* generated by  $X \in \mathfrak{X}(\mathcal{M})$ . We can prove it satisfies the condition

$$\sigma(t, \sigma^\mu(s, x_0)) = \sigma(t + s, x_0), \quad (2.31)$$

for  $s, t \in \mathbb{R}$ .

*Proof.* Since

$$\begin{aligned} \frac{d}{dt}\sigma^\mu(t, \sigma^\mu(s, x_0)) &= X^\mu(\sigma(t, \sigma^\mu(s, x_0))), \\ \sigma(0, \sigma(s, x_0)) &= \sigma(s, x_0), \end{aligned}$$

and

$$\begin{aligned} \frac{d}{dt}\sigma^\mu(t + s, x_0) &= \frac{d}{d(t+s)}\sigma^\mu(t + s, x_0) = X^\mu(\sigma(t + s, x_0)), \\ \sigma(0 + s, x_0) &= \sigma(s, x_0), \end{aligned}$$

both sides of eq. (2.31) satisfy the same ODE and the same initial condition. Then, from the uniqueness theorem for the solution of ODEs, they must be the same. ■

This leads to the following theorem.

**Theorem T.2.** *For any point  $x \in \mathcal{M}$ , there exists a differentiable map  $\sigma: \mathbb{R} \times \mathcal{M} \rightarrow \mathcal{M}$  such that*

- $\sigma(0, x) = x$ ;
- $t \mapsto \sigma(t, x)$  is a solution of (2.29) and (2.30);
- $\sigma(t, \sigma^\mu(s, x)) = \sigma(t + s, x)$ .

We're now ready to introduce Riemannian Manifold and their most relevant properties.

### 2.2.7 Riemannian Manifolds

A Riemannian Manifold is defined as a smooth Manifold which admits a Riemannian metric.

**Definition 18.** Let  $\mathcal{M}$  be a differentiable Manifold. A *Riemannian metric*  $g$  on  $\mathcal{M}$  is a type  $(0, 2)$  tensor field on  $\mathcal{M}$  such that, at each point  $p \in \mathcal{M}$ :

- $g_p(U, V) = g_p(V, U)$ ,
- $g_p(U, V) \geq 0$ , where the equality holds only when  $U = 0$ .

Here,  $U, V \in T_p\mathcal{M}$  and  $g_p = g|_p$ . Basically,  $g_p$  is a symmetric positive-definite bilinear form.

Recall the previous definition of inner product (2.22) between vectors and dual forms. For  $V \in T_p\mathcal{M}$  and  $\omega \in T_p^*\mathcal{M}$ , then  $\langle ., . \rangle: T_p^*\mathcal{M} \times T_p\mathcal{M} \rightarrow \mathbb{R}$ . If there exists a metric tensor  $g$ , then, we can use it to define the inner product between two vectors  $U, V \in T_p\mathcal{M}$ , specifically by  $g_p(U, V)$ . Since  $g_p: T_p\mathcal{M} \otimes T_p\mathcal{M} \rightarrow \mathbb{R}$ , we may define a linear map  $g_p(U, .): T_p\mathcal{M} \rightarrow \mathbb{R}$  by  $V \mapsto g_p(U, V)$ . Then, it's straightforward that  $g_p(U, .) \in T_p^*\mathcal{M}$  is a one-form. Thus, the metric  $g_p$  gives rise to an isomorphism between  $T_p\mathcal{M}$  and  $T_p^*\mathcal{M}$ .

Picking a chart  $(\varphi, U)$ , with coordinates  $\{x^\mu\}$ , we can expand the metric tensor in coordinates as

$$g_p = g_{\mu\nu}(p) dx^\mu \otimes dx^\nu, \quad g_{\mu\nu}(p) = g_p(\partial_\mu, \partial_\nu) = g_{\nu\mu}(p), \quad p \in \mathcal{M}. \quad (2.32)$$

It's usual convention to forget about the point  $p$ , denote the inverse metric as  $g^{\mu\nu}$ , and the determinant as  $\det(g_{\mu\nu}) := g$  and  $\det(g^{\mu\nu}) := g^{-1}$ . Then, the isomorphism between  $T_p\mathcal{M}$  and  $T_p^*\mathcal{M}$  can be expressed as

$$\omega_\mu = g_{\mu\nu} U^\nu, \quad U^\mu = g^{\mu\nu} \omega_\nu. \quad (2.33)$$

The purpose of the next chapter will be to rigorously define the Ricci Flow. However, to conclude this motivation part, let's take a brief detour onto string theory, in which, with a simple example in the context of non-linear sigma models, it's possible to grasp the meaning of the Ricci Flow application to understand topological properties of a Manifold through renormalization group flows in a Riemannian Manifold.

### 2.2.8 Curvature and Ricci tensor

### 2.2.9 Covariant Derivative

## 2.3 Non-Linear Sigma Models and String Theory

The standard starting point of string theory is *Polyakov action*, which describes a bosonic classical, one-dimensional, string, which describes a two-dimensional worldsheet  $\Sigma$  on a 26-dimensional spacetime described by the spacetime coordinates  $X^\mu(\xi)$ ,  $\mu = 0, \dots, 25$ , where  $\xi^a = (\tau, \sigma)$ ,  $a = 1, 2$ , are the intrinsic coordinates on  $\Sigma$ . The metric on spacetime is denoted by  $g_{\mu\nu}$ , while the metric on the worldsheet is  $\gamma_{ab}$ . For a flat spacetime, with Minkowski metric  $g_{\mu\nu} \equiv \eta_{\mu\nu} = \text{diag}(-1, +1, +1, +1)$ , the action reads

$$S_P[X^\mu(\xi), \gamma_{ab}(\xi)] = -\frac{T}{2} \int_\Sigma d\tau d\sigma \sqrt{-\det(\gamma)} \gamma^{ab} \partial_a X_\mu(\xi) \partial_b X^\mu(\xi), \quad (2.34)$$

where  $T$  is a characteristic parameter of the string, related to the string length  $l$ .

The symmetries of this action allow us to consider a flat worldsheet metric,  $\gamma_{ab} = \eta_{ab}$ , considering the so-called *unit gauge*. Then, reintroducing explicitly the metric  $g_{\mu\nu}$ , even if it's flat in this case, we obtain

$$S_P = -T \int_\Sigma d^2\xi g_{\mu\nu}(X) \partial_a X^\mu \partial^a X^\nu. \quad (2.35)$$

Basically, it represents a 2-dimensional field theory on the worldsheet, where the coordinates  $X^\mu$  are 26 dynamical fields in there. This allows us to quantize the theory with the usual quantization prescription, based on the substitution of the classical Poisson brackets defined on a symplectic manifold with the commutators of operators acting on a Hilbert space.

After quantization, one notice that, for a closed string, defined by the periodicity condition  $X^\mu(\tau, \sigma) = X^\mu(\tau, \sigma + l)$ , the particle spectrum contains a *graviton*  $\gamma_{\mu\nu}$ , which resembles a gravitational wave at low energies, a scalar field  $\varphi$  called *dilaton* and an antisymmetric two-tensor  $b_{\mu\nu}$  called *Kalb-Ramond tensor*.

Therefore, due to the presence of the graviton, one could wonder what happens for a non-flat spacetime. Then, after redefining the coordinates as a constant  $X_0^\mu$  plus some other arbitrary fields  $Y^\mu$ , i.e.,

$$X^\mu(\xi) = X_0^\mu(\xi) + \sqrt{\alpha'} Y^\mu(\xi), \quad (2.36)$$

we can expand the term in the Lagrangian as

$$g_{\mu\nu}(X)\partial_a X^\mu \partial^a X^\nu = \alpha' \left[ g_{\mu\nu}(X_0) + \sqrt{\alpha'} g_{\mu\nu,\rho}(X_0) Y^\rho(\xi) + \frac{\alpha'}{2} g_{\mu\nu,\rho\sigma}(X_0) Y^\rho(\xi) Y^\sigma(\xi) + \dots \right] \partial_a Y^\mu \partial^a Y^\nu \quad (2.37)$$

where  $g_{\mu\nu,\rho} \equiv \partial_\rho g_{\mu\nu}$ .

We obtained an expansion in  $\alpha'$ , where each term is an interaction term for the fields  $Y^\mu$ , with couplings given by the derivatives of the metric. However, a crucial symmetry of the Polyakov action (2.34) is the invariance under *conformal transformations*. Those are diffeomorphisms on a Riemannian Manifold which preserve the metric up to rescaling, i.e.,

$$g(x) \rightarrow \tilde{g}(\tilde{x}) = e^{2\omega(\tilde{x})} g(\tilde{x}). \quad (2.38)$$

Without going into the details, the presence of this symmetry is considered as a consistency condition for the theory, as it allows for a perturbative interpretation of the interactions. In addition, the above interacting quantum field theory must undergo renormalization, in order to cure the divergences.

However, after renormalization, the conformal symmetry may be anomalous<sup>2</sup>. Indeed, a particular example of conformal transformation (2.38) is provided by scale-invariance. That is to say, the theory can't depend on a scale to be conformal invariant. But, as the methods of *renormalization group* teach us, after renormalization the couplings run with the energy scale  $M$  of the system, dependence which is encapsulated into the  $\beta$ -function

$$\beta(g_{\mu\nu}) = M \frac{\partial}{\partial M} g_{\mu\nu}. \quad (2.39)$$

As a consequence, for a quantum string theory to make sense, it must be conformal invariance, so the  $\beta$ -function associated to the metric, in the action (2.35) with the expansion (2.37), must vanish

$$\beta(g_{\mu\nu}) \stackrel{!}{=} 0. \quad (2.40)$$

A similar argument can be pursued for the other two particles in the closed string spectrum, i.e., the dilaton  $\varphi$  and the Kalb-Ramond form  $b_{\mu\nu}$ . The corresponding action will be

$$S_\sigma = -\frac{T}{2} \int_{\Sigma} d^2\xi \sqrt{-\det(\gamma)} [(\gamma^{ab} g_{\mu\nu}(X) + i\varepsilon^{ab} b_{\mu\nu}(X)) \partial_a X^\mu \partial_b^\nu + \alpha' \mathcal{R}\varphi(X)], \quad (2.41)$$

---

<sup>2</sup>An anomaly is a classical symmetry which is not preserved at the quantum level. In particular, it is due to a non-invariance of the measure of the path integral.

where  $\varepsilon^{ab}$  is the 2d Levi-Civita symbol, while  $\mathcal{R} = \mathcal{R}(\gamma)$  is the Ricci scalar on the worldsheet.

Defining the Field Strength  $H_{\mu\nu\rho} = \partial_\mu b_{\nu\rho} + \partial_\nu b_{\rho\mu} + \partial_\rho b_{\mu\nu}$ , the vanishing of the beta functions reads

$$\beta(g_{\mu\nu}) = \alpha' \left( R_{\mu\nu} - \frac{1}{4} H_{\mu\lambda\rho} H^{\mu\lambda\rho} + 2 \nabla_\mu \nabla_\nu \varphi \right) + O(\alpha'^2) \stackrel{!}{=} 0, \quad (2.42a)$$

$$\beta(b_{\mu\nu}) = \alpha' \left( \frac{1}{2} \nabla^\rho H_{\rho\mu\nu} + \nabla^\rho \varphi H_{\rho\mu\nu} \right) + O(\alpha'^2) \stackrel{!}{=} 0, \quad (2.42b)$$

$$\beta(\varphi) = \alpha' \left( \frac{1}{2} \nabla_\mu \varphi \nabla^\mu \varphi - \frac{1}{2} \nabla^2 \varphi - \frac{1}{24} H_{\mu\nu\rho} H^{\mu\nu\rho} \right) + O(\alpha'^2) \stackrel{!}{=} 0. \quad (2.42c)$$

The above equations are constraints for the spacetime fields  $(g, b, \varphi)$ , imposed to preserve conformal invariance of the quantum string. However, since those fields should be dynamical on spacetime, those must also be their equations of motion. This leads to the following *low-energy effective action*, which has (2.42) as equations of motion

$$S_{26} = \frac{1}{k_0^2} \int d^{26}x \sqrt{\det(g)} e^{-2\varphi} \left( \mathcal{R}(g) - \frac{1}{12} H_{\mu\nu\rho} H^{\mu\nu\rho} + 4 \nabla_\mu \varphi \nabla^\mu \varphi \right). \quad (2.43)$$

To set this problem to a more general ground, and understand how this model is related to Ricci Flow, let's define more accurately what a  $\sigma$ -model is in field theory. A  $\sigma$ -model is a field theory for a field  $\Phi: \Sigma \rightarrow \mathcal{M}$  that takes values in a manifold  $\mathcal{M}$ . Traditionally,  $\Sigma$  is the spacetime on which the field theory lives, and  $\mathcal{M}$  is called the target space. If the target space carries some linear structure, like a vector space, then the whole physical system is called a linear  $\sigma$ -model. For general manifolds such as generic Riemannian ones, it is then called a non-linear  $\sigma$ -model. What we did above is to study the  $\sigma$ -model spacetime renormalization effects on the target space  $\mathcal{M}$ , and this is indeed an instance of Ricci Flow.

## 2.4 Ricci Flow to Tackle Topological Problems



# CHAPTER 3

## RICCI FLOW AND OLIVER-RICCI CURVATURE

---

Initially introduced by Richard S. Hamilton in the early 1980s, Ricci Flow arose historically as a powerful method in differential geometry. At its heart, it seeks to “smooth out” geometric irregularities of manifolds by evolving the underlying Riemannian metric through a partial differential equation (PDE) reminiscent of the classical heat equation. We recall that a manifold is a topological space locally resembling Euclidean space, and a *Riemannian manifold* is such a space equipped with an inner product on each tangent space, making it possible to measure angles, distances, and curvature.

Curvature, in particular, is fundamental to geometry: it describes how space bends or deviates from flatness. On a two-dimensional surface embedded in three-dimensional space, for example, curvature can be visualized by examining the deviation of geodesics (the generalization of “straight lines” in curved spaces) from parallelism, or by looking at how areas or angles are distorted compared to those in flat Euclidean geometry. The extension to higher dimensions and more abstract manifolds involves careful definitions but retains this key notion of “spatial bending.”

### 3.1 Riemannian Geometry and Curvature Notions

In classical Riemannian geometry, curvature can be examined from multiple perspectives. One can study the *sectional curvature*, which measures how a two-dimensional plane (spanned by two tangent directions) curves. One can also investigate the *Ricci curvature*, which is obtained by summing or averaging the sectional curvatures over all planes containing a given direction. Ricci curvature has special importance: for instance, it appears in Einstein’s equations of General Relativity, linking geometry to matter and energy distributions in spacetime.

Concretely, let  $(M, g)$  be a Riemannian manifold, where  $M$  is a smooth manifold and  $g$  is the metric tensor. The Ricci curvature  $\text{Ric}$  is derived as a contraction of the Riemann curvature tensor, itself an operator capturing how much nearby geodesics converge or diverge. Positive Ricci curvature typically implies that geodesics tend to converge, reflecting a “crowded” or positively curved geometry akin to the sphere. Negative Ricci curvature implies geodesics tend to diverge, mirroring a hyperbolic or “saddle-like” structure. Zero Ricci curvature is the hallmark of Ricci-flat manifolds, with many implications for geometry and topology.

### 3.1.1 Hamilton’s Ricci Flow Equation

Hamilton introduced the Ricci Flow as the PDE:

$$\frac{\partial g_{ij}}{\partial t} = -2 R_{ij},$$

where  $g_{ij}$  are the components of the metric tensor  $g$  in local coordinates and  $R_{ij}$  are the components of the Ricci curvature tensor. Informally, each infinitesimal piece of the manifold changes in time, guided by curvature. Regions of *high positive* Ricci curvature shrink faster, while regions of *negative* Ricci curvature expand. This leads to a *flow* that tends to smooth out the geometric and topological features of  $M$ .

One of the most famous applications of Ricci Flow on manifolds is Grigori Perelman’s resolution of the Poincaré Conjecture and the more general Geometrization Conjecture for three-dimensional manifolds. Perelman’s work introduced the notion of *Ricci Flow with surgery*, a procedure to remove singular regions (places where curvature blows up to infinity) and continue the flow on the remaining parts. In 3D manifolds, these singularities can be visualized as “neck pinches” that effectively separate the manifold into topologically simpler pieces. Perelman showed that by performing a series of well-defined surgeries, one could decompose a three-dimensional manifold into model geometric pieces, completing Hamilton’s program toward a proof of the Geometrization Conjecture.

### 3.1.2 From Smooth Settings to Discrete Geometry

While Ricci Flow is classically defined on smooth manifolds, there has been considerable interest in transferring these ideas to *discrete* or combinatorial settings such as polyhedral surfaces, graphs, and complex networks. The general question is how to define concepts like “curvature” when one does not have a smooth manifold or a

Riemannian metric in the usual sense. Instead, discrete analogs focus on adjacency, distances along edges, and combinatorial properties that mimic or reflect continuum notions.

For surfaces composed of polygons (triangulations), one can define the curvature at a vertex via angle deficits, a concept dating back to classical differential geometry of polyhedral surfaces. However, for higher-dimensional graphs and networks that are not neatly embedded in any Euclidean space, a more general curvature definition is needed—one that depends mostly on the underlying distances and probability measures rather than an explicit embedding.

## 3.2 Optimal Transport and Ollivier's Ricci Curvature

A major breakthrough in defining a curvature notion for general metric spaces (including discrete networks) came via *optimal transport*. Historically, the optimal transport problem, originating in the work of Gaspard Monge in the 18th century, asks how to map one mass distribution into another with minimal transportation cost. Subsequent reformulations by Leonid Kantorovich turned this into a linear optimization problem known as the *Kantorovich relaxation*.

If  $(X, d)$  is a metric space, and we have two probability measures  $\mu$  and  $\nu$  on  $X$ , the *Wasserstein distance* (also called the earth mover's distance) measures how much "effort" is needed to move mass from  $\mu$  to  $\nu$ , given the metric  $d$ . Specifically, one solves an optimization problem that tries to minimize the total cost of moving infinitesimal amounts of mass from one location to another.

Yann Ollivier harnessed this framework to define a notion of *coarse Ricci curvature* on general metric measure spaces. Ollivier's definition, now widely called *Ollivier Ricci curvature*, is based on considering small probability balls of radius  $\varepsilon$  around points (or sometimes discrete probability measures concentrated on nearest neighbors in a graph) and calculating how much these small balls cost to move one onto the other under optimal transport. If moving these balls requires comparatively more effort than just their pairwise distance would suggest, the edge or connection between them is deemed negatively curved; if it requires less effort, it is positively curved. This emerges from an analog of the well-known statement in Riemannian geometry that Ricci curvature controls how geodesic balls deviate from each other, which can be recast in terms of mass transport.



# CHAPTER 4

## APPLICATION TO COMPLEX NETWORKS

---

To adapt Ollivier's construction to a graph  $G = (V, E)$  where  $V$  is the set of nodes and  $E$  is the set of edges (possibly with weights), one often assigns to each node  $x$  a probability measure  $m_x$ . A typical choice is to concentrate the mass uniformly on  $x$ 's neighbors, possibly with some parameter  $\alpha$  to keep a fraction of the mass at  $x$  itself. Let  $W(m_x, m_y)$  denote the Wasserstein distance between  $m_x$  and  $m_y$ . The Ollivier Ricci curvature  $\kappa(x, y)$  along the edge  $(x, y)$  is defined as

$$\kappa(x, y) = 1 - \frac{W(m_x, m_y)}{d(x, y)},$$

where  $d(x, y)$  is the usual shortest-path distance (or a weight-based distance) between  $x$  and  $y$ . Intuitively:

- If many of the neighbors of  $x$  align well with the neighbors of  $y$ , then  $W(m_x, m_y)$  is relatively small compared to  $d(x, y)$ , giving a larger curvature.
- If the neighbors do not overlap much,  $W(m_x, m_y)$  will be comparatively large, implying smaller (or possibly negative) curvature.

This lines up with the idea that a highly "clustered" or cohesive set of nodes—often indicating an underlying community—acts more like a positively curved region in the manifold analogy, whereas edges bridging distant clusters reflect negative curvature. These insights lead to a method for analyzing and partitioning networks by focusing on edges with specific curvature characteristics.

## 4.1 ARI, Modularity, and Performance

In the study of complex networks, a fundamental task is to identify densely connected groups of nodes, commonly referred to as *communities*. These communities often correspond to meaningful substructures such as friend groups in social networks, functionally related proteins in biological networks, or topics in citation networks. There are numerous algorithms that aim to extract communities—ranging from graph partitioning heuristics and centrality-based edge removal to statistical and probabilistic methods.

The Ricci Flow-based technique for network community detection focuses on the geometric viewpoint: an edge with significantly negative Ricci curvature may signify a *bridge* between distinct communities, whereas edges with positive curvature are typically nestled within cohesive communities. Iteratively adjusting edge weights according to Ollivier Ricci curvature has the effect of “magnifying” bridging edges and “contracting” internal edges, ultimately making a subsequent threshold-based cut reveal the inherent clusters.

Here are the major steps (in broad terms) for using Ricci Flow to detect communities:

1. **Initialization:** Assign an initial weight to each edge  $(x, y)$ . Often, one starts with uniform weights or with weights based on an existing property such as adjacency or similarity.
2. **Probability Measures:** Choose how to define the measure  $m_x$  at each node  $x$ . A popular simple choice is to put uniform weight on all neighbors of  $x$ , ensuring  $\sum_{v \in \text{neighbors}(x)} m_x(v) = 1$ . Other weighting schemes (e.g., discounting more distant neighbors) can also be used.
3. **Curvature Computation:** For each edge  $(x, y)$ , compute the Ollivier Ricci curvature  $\kappa(x, y)$  by solving the discrete optimal transport problem and using

$$\kappa(x, y) = 1 - \frac{W(m_x, m_y)}{d(x, y)}.$$

4. **Discrete Ricci Flow Update:** Adjust the edge weight according to

$$w_{xy}^{(i+1)} = w_{xy}^{(i)} - \eta \kappa_{xy}^{(i)} d_{xy}^{(i)}.$$

Often, one sets  $\eta = 1$  and updates all edges simultaneously, then recomputes shortest path distances  $d(\cdot, \cdot)$  for the next iteration. The total number of iterations can be chosen based on convergence criteria or practical heuristics.

5. **Network Surgery:** After a certain number of iterations, examine the distribution of edge weights. Typically, bridging edges (those connecting separate communities) will have grown in length. Choose a threshold  $T$  such that edges with  $w_{xy} > T$  are considered “cuts,” removing them from the graph. The connected components that remain are taken as the identified communities.
6. **Post-Processing:** If a graph has hierarchical communities, additional steps (e.g., repeating the process within subcomponents) might be performed to further subdivide the clusters.

This pipeline is quite flexible in terms of parameter choices (e.g., the measure definition, the number of flow iterations, the threshold for edge cuts) and can adapt to various network topologies. The next subsections explain how to measure the resulting partition quality, focusing on two widely employed tools: the *Adjusted Rand Index (ARI)* and *Modularity*.

### 4.1.1 Adjusted Rand Index (ARI)

#### General Definition

The *Adjusted Rand Index (ARI)* is a popular external validation measure to compare a discovered clustering with a known ground-truth partition. Suppose you have a set of  $n$  items (in our case, the  $n$  nodes of a network). Let  $C = \{C_1, \dots, C_r\}$  be a partition of these items into  $r$  clusters found by some method, and let  $G = \{G_1, \dots, G_s\}$  be the ground-truth (or reference) partition into  $s$  clusters. The Rand Index (RI) measures the fraction of item pairs that are *consistently* assigned in both partitions (i.e., either assigned together in both or assigned to different clusters in both).

Formally, the Rand Index is given by:

$$\text{RI}(C, G) = \frac{a + d}{a + b + c + d},$$

where

- $a$  is the number of pairs of items that are in the same cluster in  $C$  *and* in the same cluster in  $G$ ,

- $b$  is the number of pairs of items that are in the same cluster in  $C$  but in different clusters in  $G$ ,
- $c$  is the number of pairs that are in different clusters in  $C$  but in the same cluster in  $G$ ,
- $d$  is the number of pairs that are in different clusters in  $C$  and in different clusters in  $G$ .

Because  $a + d$  counts all the agreements (put together or kept apart) and  $b + c$  counts the disagreements,  $\text{RI}(C, G)$  is between 0 and 1, with 1 meaning a perfect match of the partitions.

However, the Rand Index does not correct for chance agreement. The *Adjusted Rand Index* refines this by subtracting the expected RI of random partitions and rescaling. One can define:

$$\text{ARI}(C, G) = \frac{\text{RI}(C, G) - \text{Expected}[\text{RI}]}{\max(\text{RI}) - \text{Expected}[\text{RI}]},$$

which yields a value that ranges from 0 (or negative, depending on definition) up to 1. Here, 1 indicates the clustering  $C$  exactly matches the ground-truth  $G$ , whereas an ARI near 0 suggests random agreement.

### Applying ARI to Ricci Flow-based Community Detection

When applying Ricci Flow on a network, one typically obtains a final partition of the graph by removing edges beyond a certain length. If a ground-truth labeling exists, we compute the ARI to assess how well these communities align with the reference. If ARI is high, that means the geometric approach successfully captured the intended grouping. By examining the ARI as a function of the threshold, one can also decide the best cutoff for the “network surgery.” In practice, one might do a range of threshold values, measure the ARI for each, and pick the threshold that maximizes it (assuming the ground-truth is known). In contexts where the ground-truth partition is not known, we might rely on internal validation measures, such as modularity, to guess a suitable threshold.

#### 4.1.2 Modularity

##### Definition of Modularity

*Modularity* is one of the most commonly used internal metrics for community detection in networks. Proposed initially by Newman and Girvan, it quantifies how

well a particular partition of the network divides the nodes into communities that are dense internally and sparse between each other.

Let us consider a network with  $n$  nodes and  $m$  edges (or total edge weight if it is a weighted graph). For a given partition of the network into  $k$  communities, the modularity  $Q$  is computed as:

$$Q = \frac{1}{2m} \sum_{i,j} \left( A_{ij} - \frac{d_i d_j}{2m} \right) \delta(c_i, c_j),$$

where  $A_{ij}$  is the adjacency matrix (or the weight matrix),  $d_i$  is the degree (or sum of weights) of node  $i$ ,  $c_i$  is the community label of node  $i$ , and  $\delta(c_i, c_j)$  is 1 if  $i$  and  $j$  are in the same community and 0 otherwise. The term  $\frac{d_i d_j}{2m}$  approximates the expected number of edges (or expected weight) between  $i$  and  $j$  if edges are distributed randomly but respect node degrees. High modularity indicates that the actual number of intra-community edges is significantly above random expectation.

### Modularity as a Stopping or Surgery Criterion

When using Ricci Flow for community detection, one can track how modularity evolves as edges get re-weighted and as one tries different thresholds for cutting. Typically, there is an intuitive sweet spot where further cutting does not substantially improve the modularity and might begin to over-segment the network.

A practical strategy is as follows:

1. Perform a fixed number of Ricci Flow iterations.
2. For a range of potential cut thresholds  $T_1, T_2, \dots, T_r$ , remove edges with weight above  $T_j$ .
3. Compute modularity  $Q_j$  for each  $T_j$ .
4. Select the threshold  $T_j$  that yields the maximum  $Q_j$  preceding a drop in modularity.

This threshold selection process is akin to the notion of “neck pinches” or “surgeries” in the manifold setting: a large weight often signifies a bridging structure (negative curvature region grown large) that is “pinching off” from the main components. If an external ground-truth is known, one may prefer the threshold that simultaneously optimizes ARI and modularity. In the absence of external labels, maximizing modularity is a common choice to define the “best” partition.

### 4.1.3 Interpreting Network “Surgery” in This Context

A hallmark of the classical Ricci Flow with surgery on manifolds is that when the flow develops singularities (often visualized as “neck pinches”), the manifold is physically separated into topologically distinct pieces. Drawing an analogy, in discrete Ricci Flow on graphs, the edges that grow large (due to negative curvature) can be viewed as “singularities” or bridging regions, reminiscent of the neck that pinches in a continuous manifold. The act of removing these edges at some iteration is the direct analog of performing surgery on the manifold. After removing these “necks,” the graph breaks into connected components, each presumably representing a dense or well-curved subregion, i.e., a community.

In practice, we carry out this network surgery step once or multiple times, balancing the preservation of meaningful connectivity with the desire to isolate truly separated clusters. Because many real networks can exhibit hierarchical or multi-level community structures, it is possible that each sub-component can be further refined if we continue the process within it. This multi-scale approach can be repeated if one suspects nested communities.

### 4.1.4 Algorithmic Complexity and Practical Considerations

While the continuous Ricci Flow PDE can be computationally demanding in the smooth case, the discrete version has its own set of computational challenges. The major cost typically arises in:

1. **Wasserstein Distances:** Computing  $W(m_x, m_y)$  for each edge  $(x, y)$ . In a graph with  $n$  nodes and  $e$  edges, if we attempt an exact solution of the optimal transport problem, it can become computationally expensive. However, in many practical discrete settings, especially with local probability measures  $m_x$  that concentrate mass on immediate neighbors,  $W(m_x, m_y)$  can often be computed with simpler combinatorial formulas or approximations.
2. **Repeated Distance Computation:** After each iteration, we update edge weights and potentially must recompute shortest-path distances  $d(x, y)$  for all node pairs or for edges. If  $e$  is large, repeated all-pairs computations might be costly, unless efficient incremental shortest-path algorithms or approximate methods are used.

Despite these costs, modern computational resources and heuristics usually make discrete Ricci Flow feasible for networks of moderate size. For very large networks

(millions of edges), one might rely on approximations, sampling techniques, or simplified versions of curvature (e.g., proxies to Ollivier Ricci curvature).

In practice, one needs to choose three important parameters:

1. **Number of Ricci Flow Iterations:** Stopping too soon might not emphasize bridging edges enough to isolate communities; iterating too long might lead to degeneracies (e.g., certain edges become extremely large or extremely small). An empirical strategy is to run a moderate number (e.g., 10–20 iterations) and check if measures like ARI (if a ground truth is available) or modularity saturate.
2. **Cut Threshold for Network Surgery:** Typically chosen by scanning multiple thresholds and evaluating a measure of clustering quality (e.g., modularity) or ARI.
3. **Mass Distributions:** The simplest is uniform distribution on neighbors (sometimes with or without a fraction of mass at the node itself). More sophisticated distributions might downweight distant neighbors, especially in large or weighted networks.

#### 4.1.5 Broader Theoretical Context and Future Directions

From a more theoretical vantage point, *why* does curvature—in the sense of Ollivier—detect communities so well? Intuitively, the geometry of a manifold with positive curvature is reminiscent of a cohesive, “ball-like” region, while negatively curved regions show hyperbolic expansions akin to branching. In network terms, cohesive subgraphs correspond to a “positive curvature signature” because local random walks or local mass distributions align more easily, whereas bridging edges or tree-like expansions create a negative curvature effect.

Future directions could include:

- Exploring *Forman-Ricci* curvature or other discrete curvature notions to see how they compare in community detection or anomaly detection tasks.
- Combining *higher-order* or *simplicial* network topologies, in which edges, triangles, and higher-dimensional simplices each carry a curvature notion, potentially refining the detection of substructures.
- Investigating multi-scale or hierarchical surgery, systematically refining each sub-community using iterative curvature-based updates.

All of these highlight that curvature-based community detection offers a distinctive geometric lens on networks, bridging rich ideas from differential geometry to the realm of data science and large-scale graph analysis.

# CHAPTER 5

## THE DEVELOPED CODE

---

The objectives of the developed code were

- **Implementation of a Ricci Flow method** able to evaluate the Ollivier-Ricci curvature of a given graph and update its edges' weights accordingly. Then we wanted the method to perform surgery on weakly connected edges to allow for community detection.

For these purposes we relied on Ollivier-Ricci library developed by Ni et al. [3], see [section 5.1](#).

- **Plotting graphs and communities** to appreciate the behavior of the method and obtain graphical results.
- **Testing the method** on synthetic graphs, trying to benchmark with an analogue test made by Ni et al. [8]. Results and further details are given in [section 5.2](#).
- **Evaluation of performances** by comparing the method with other commonly used community detection methods.
- **Application on real world data.** To do this we chose Zachary's Karate Club graph, which is directly accessible from Networkx library. Results and further details are given in [section 5.3](#).

In the this chapter we present the main ideas and tools related to the code. To get more insights on how the code as been constructed and subdivided (i.e. various classes and functions) we recommend consulting [CodeDocumentation](#) or the GitHub of the whole project: [RicciFlowNetwork](#).

## 5.1 The setup

To facilitate the computation of Ricci curvature within networks, we made use of the GraphRicciCurvature library as our starting point. This Python library is part of a more comprehensive library on Ricci curvature for networks. The latter provides tools to compute two discrete Ricci curvatures: Ollivier-Ricci and Forman-Ricci; it supports the analysis of both weighted and unweighted graphs. In addition, it offers basic methods for graph surgery and evaluation of the *adjusted rand index* (ARI).

Each graph we employed was generated with Networkx library. We also used its methods as a starting point for graphical representations. For plotting we implemented `GraphDrawer` class which, among other functionalities, allows us to see the detected communities separated in subgraphs. Nodes are colored with their corresponding community color, giving a visual indication of method's performance.

We used this setup to implement the code workflow depicted in fig. 5.1.

## 5.2 Tests on Synthetic Graphs

### 5.2.1 Stochastic Block Model Test Graph

To start testing our code we choose a Stochastic Block Model (SBM) graph. A SBM graph is a type of random graph model used to generate networks with a predefined community structure. It is an extension of the Erdos–Rényi, where nodes are divided into communities, and the probability of an edge between two nodes depends on their community membership. It is characterized by  $N$  nodes,  $k$  communities and a connectivity matrix  $P_{ij}$  which represents the probability of an edge between a node in community  $i$  and a node in community  $j$ . Since communities are predefined when generating the graph, we can directly compare the detected communities with the true ones.

For our test we set

$$N = 500, \quad k = 2, \quad P = \begin{bmatrix} 0.20 & 0.03 \\ 0.03 & 0.20 \end{bmatrix}$$

with every initial weight equal to one.

Curvature values for the initial SBM graph are shown in fig. 5.2a, while on the right we have the updated curvatures after 10 iterations of Ricci Flow. We can see that the community structure of this graph is already well established; Ricci Flow has however

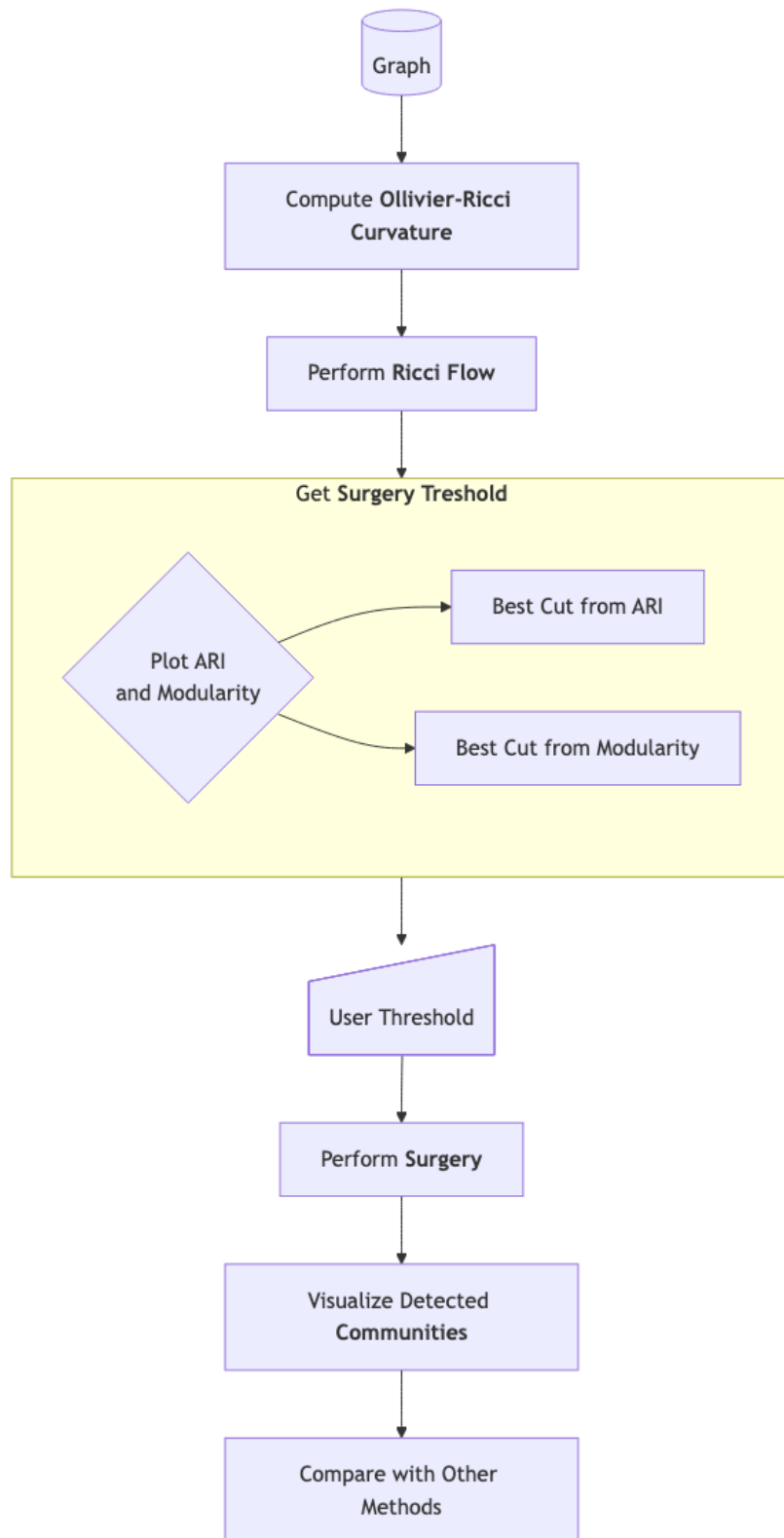


Figure 5.1 Code workflow.

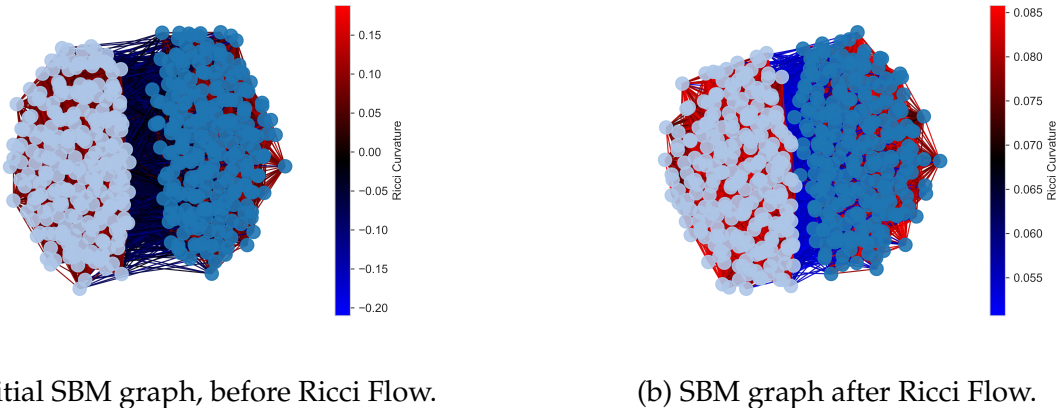


Figure 5.2 Comparison of SBM graph before and after having applied 10 iterations of Ricci Flow on edges.

highlighted the weak connection of central inter community nodes as one can see in fig. 5.2b.

In fig. 5.3 we see that surgery with a cutoff between 1 and  $\approx 1.5$  leads to a perfect distinction between the two communities, i.e. an ARI of 1.

Lastly, fig. 5.4a depicts the graph after surgery with a cutoff between 1 and  $\approx 1.5$ . As expected we got a separation into two distinct clusters. Fig. 5.4b shows the two communities corresponding to the two connected components.

### 5.2.2 Lancichinetti-Fortunato-Radicchi Test Graph

As a more complex synthetic graph for testing we used a Lancichinetti-Fortunato-Radicchi (LFR) benchmark graph. LFR graphs are widely used for testing community-detection algorithms because they produce networks with heterogeneous (scale-free) degree distributions and community-size distributions, making them more realistic than simpler models. Nodes are assigned to communities according to specified power-law exponents, and a “mixing” parameter controls the fraction of edges that connect different communities.

For our test we built a graph with 500 nodes ( $n = 500$ ) with a degree distribution exponent  $\tau_1 = 3$  and a community-size exponent  $\tau_2 = 1.5$ . For the mixing parameter we chose  $\mu = 0.2$  indicates a relatively strong community structure by limiting the proportion of inter-community edges. We set each community to have a minimum of 20 nodes and a maximum of 70 nodes. The expected average degree is set to 20, with a maximum node degree capped at 50.

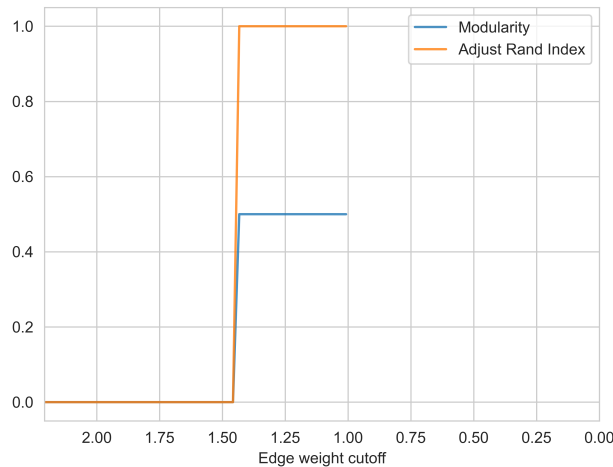


Figure 5.3 SBM graph's ARI and modularity behavior for different surgery cutoffs.

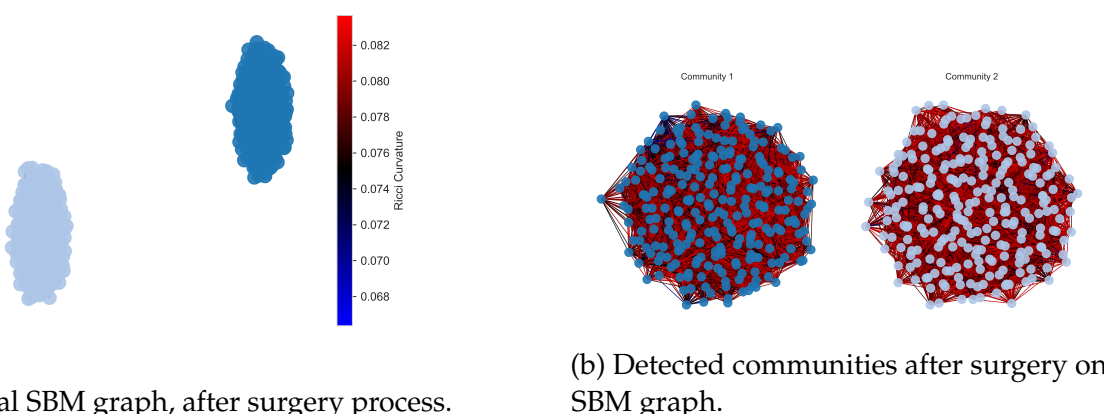


Figure 5.4 Comparison of SBM graph after surgery and corresponding connected components (i.e. the detected communities).

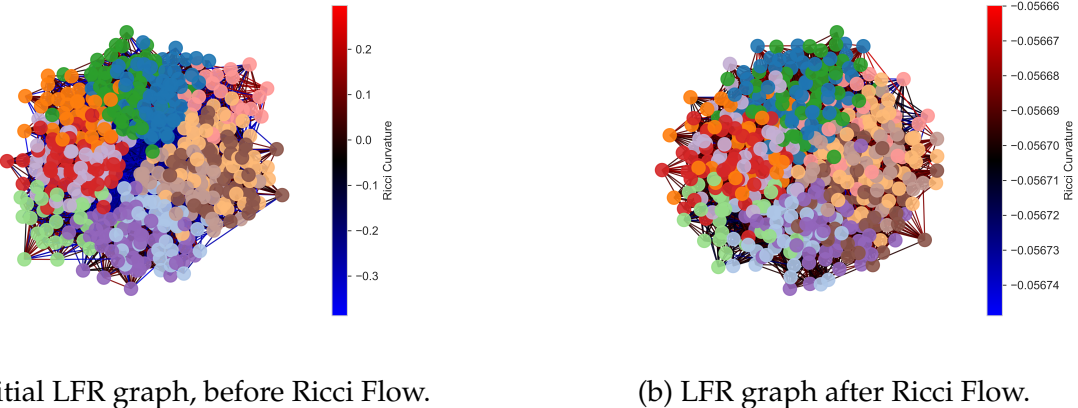


Figure 5.5 Comparison of LFR graph before and after having applied 40 iterations of Ricci Flow on edges.

For this graph we applied 40 iterations of Ricci Flow as its structure is more complex than the previous SBM graph (see fig. 5.5a). In fig. 5.5b we see a convergence of the curvature values after Ricci Flow; the high number of nodes and communities makes difficult to visualize properly the graph, for this reason we introduced also an histogram plot of weights and curvature values in the final code implementation for the Karate club graph (see section 5.3).

Fig. 5.6 shows the behavior of ARI and modularity depending on the chosen cutoff point. Also in this case we see that it is possible to obtain an ARI of 1.

In fig. 5.7 we have the graph after surgery (we chose as cutoff  $\approx 1.12$  to get an ARI of 1) and we can see that it got divided into connected components with all the nodes of the same color, i.e. same community. In this case we did not produce a plot community by community due to the high number of clusters.

### 5.2.3 Further Tests on Lancichinetti-Fortunato-Radicchi Graphs

As a final test for our code we decided to try reproducing a result presented in the work of Ni et al. [8] (see figure 8a at page 12). In particular, it is about applying Ricci Flow on different LFR graphs differing for the modularity parameter  $\mu$ . Of course one expects the ARI to decrease with increasing values of  $\mu$  as the community structure becomes less defined.

In fig. 5.8 we present our results with OTD method for curvature evaluation using first OTD and then ATD

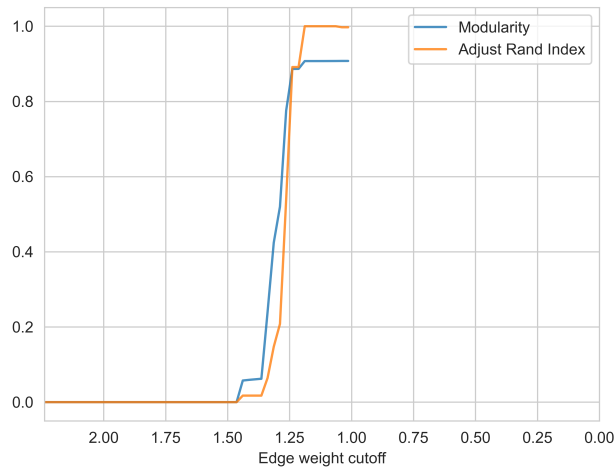


Figure 5.6 LFR graph's ARI and modularity behavior for different surgery cutoffs.

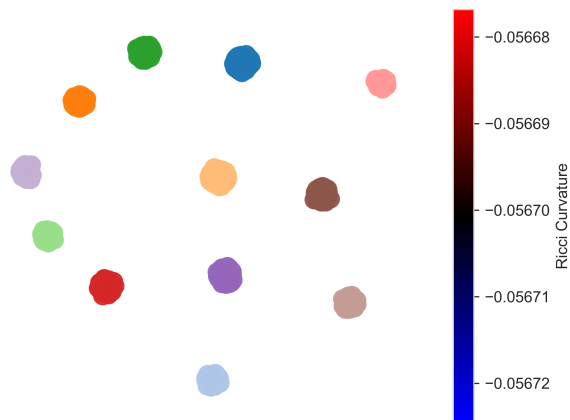


Figure 5.7 Final LFR graph, after surgery process.

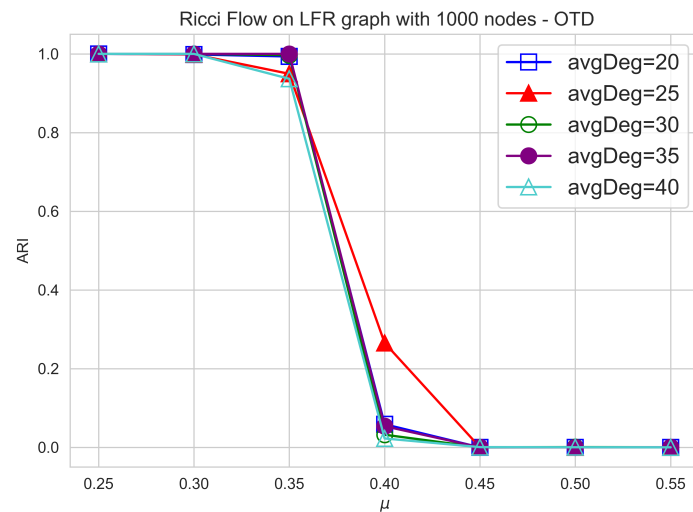


Figure 5.8 LFR OTD

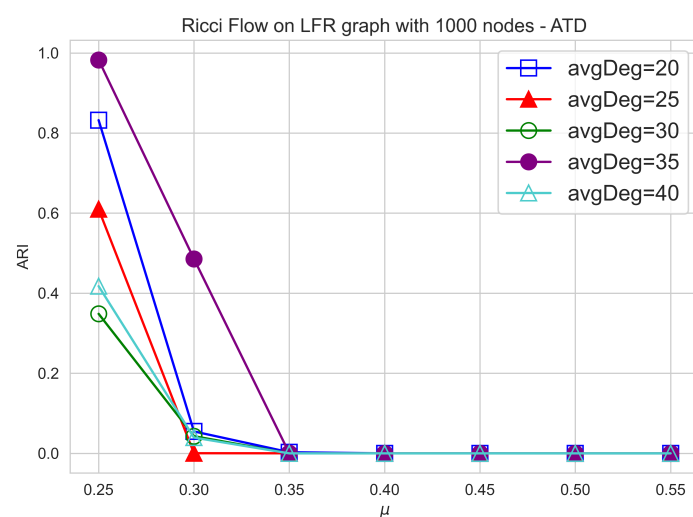
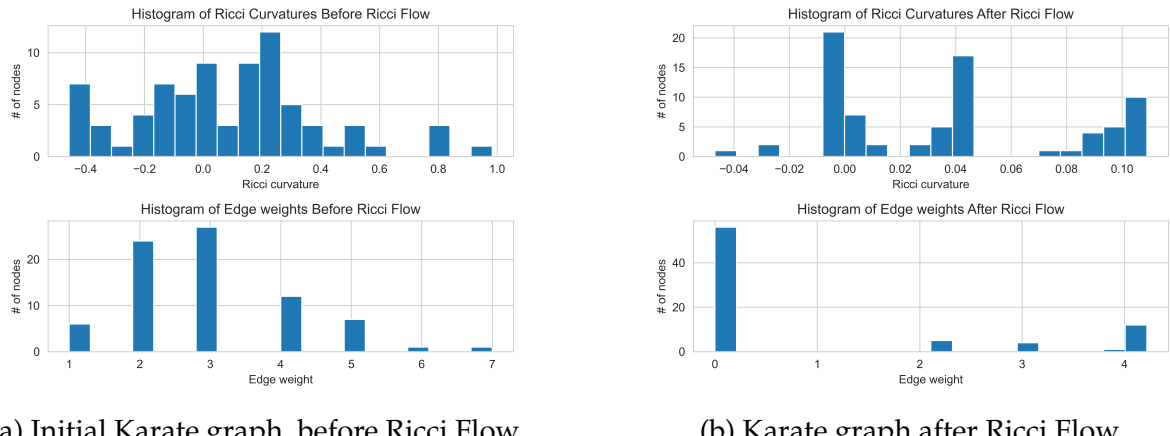


Figure 5.9 LFR ATD



(a) Initial Karate graph, before Ricci Flow.

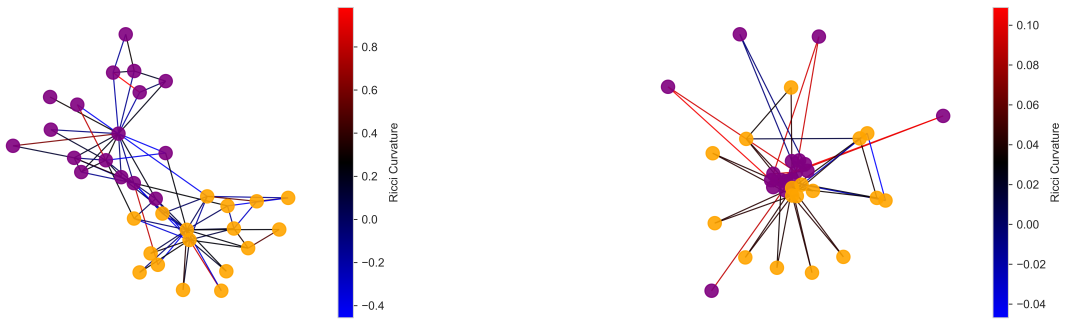
(b) Karate graph after Ricci Flow.

Figure 5.10 Comparison of curvature values and weights before and after having applied Ricci Flow on edges.

Our graphs do not match exactly the plots of Ni et al., as for them the loss of ARI starts from higher values of  $\mu$ . This could be for various reasons:

- It is unclear which parameter they used to generate LFR graphs. For example, using Networkx it is not possible to control exactly the number of communities (only a minimum and maximum number can be set), so they probably generated their graphs in a different but unspecified way.
- They used an average ARI, probably generating the same graph multiple times. We generated the graph and applied the Ricci Flow just once due to an already high execution time.
- Their surgery process it is not specified in detail. They might have used multiple surgeries over the same Ricci Flow process to remove possible singularities affecting the final performance (even though this should not be the case for this kind of graph).

## 5.3 Application to Zachary's Karate Club Graph



(a) Initial Karate graph, before Ricci Flow.

(b) Karate graph after Ricci Flow.

Figure 5.11 Comparison of Karate graph before and after having applied Ricci Flow on edges.

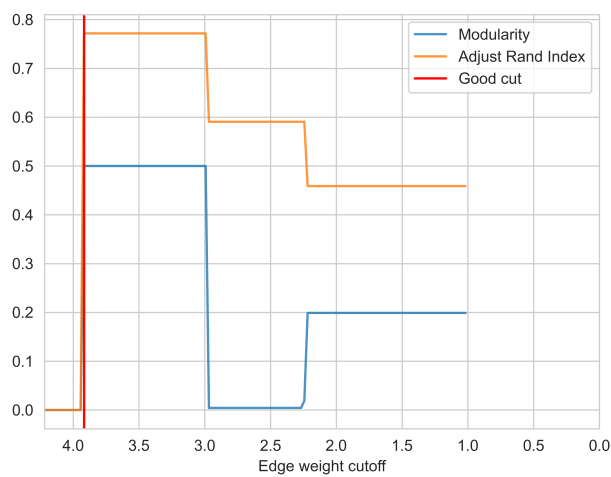


Figure 5.12 Karate acc

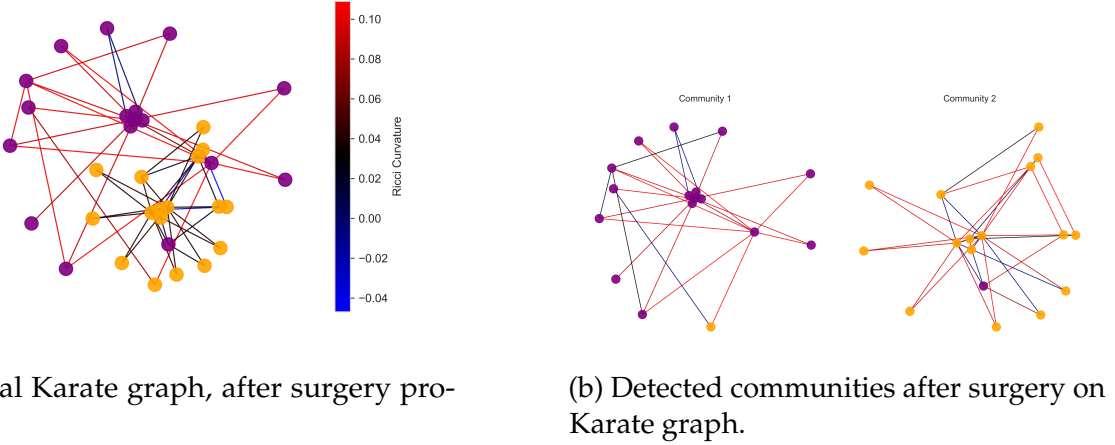


Figure 5.13 Comparison of Karate graph after surgery and corrensponding connected components (i.e. the detected communities).

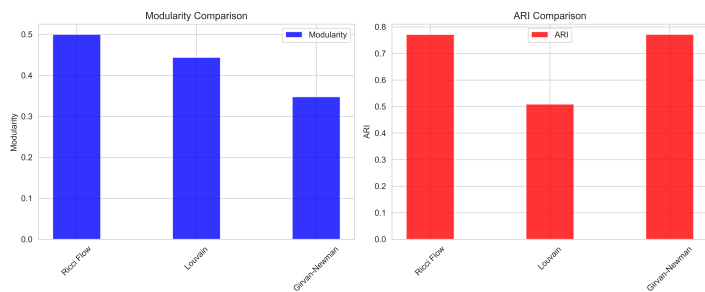


Figure 5.14 Karate acc



# CHAPTER 6

## CONCLUSIONS AND FUTURE DIRECTIONS

---



## APPENDIX A

### METRIC OF A 2-SPHERE

---



## REFERENCES

---

- [1] Richard H Bamler. “Recent developments in Ricci flows”. In: (2021). arXiv: [2102.12615 \[math.DG\]](https://arxiv.org/abs/2102.12615). URL: <https://arxiv.org/abs/2102.12615>.
- [2] Mauro Carfora et al. “Ricci Flow from the Renormalization of Nonlinear Sigma Models in the Framework of Euclidean Algebraic Quantum Field Theory”. In: (2019). arXiv: [1809.07652 \[math-ph\]](https://arxiv.org/abs/1809.07652). URL: <https://arxiv.org/abs/1809.07652v2>.
- [3] Ni C.C., Cruceru C., and Barrett S. *GraphRicciCurvature*. <https://github.com/saibalmars/GraphRicciCurvature.git>. 2019.
- [4] B. Chow and D. Knopf. *The Ricci Flow: An Introduction*. American Mathematical Society, 2004. ISBN: 0-8218-3515-7.
- [5] Martin D. Crossley. *Essential Topology*. Springer, 2005. DOI: [10.1007/1-84628-194-6](https://doi.org/10.1007/1-84628-194-6).
- [6] Lee J. M. *Introduction to Riemannian Manifolds*. Second Edition. Springer, 2018. DOI: [10.1007/978-3-319-91755-9](https://doi.org/10.1007/978-3-319-91755-9).
- [7] Lee J. M. *Introduction to Smooth Manifolds*. Second Edition. Springer, 2013. DOI: [10.1007/978-981-99-0565-2](https://doi.org/10.1007/978-981-99-0565-2).
- [8] Chien-Chun Ni et al. “Community Detection on Networks with Ricci Flow”. In: (2019). arXiv: [1907.03993 \[cs.SI\]](https://arxiv.org/abs/1907.03993). URL: <https://arxiv.org/abs/1907.03993>.
- [9] Henri Poincaré. “Analysis Situs”. Trans. by John Stillwell. In: *Journal de l’École Polytechnique* 2 (1895).
- [10] Henri Poincaré. “Cinquième complément à l’analysis situs”. Fifth Complement to Analysis Situs. Trans. by John Stillwell. In: *Rendiconti del Circolo Matematico di Palermo* 18 (1904 2008), pp. 45–110.
- [11] J. Polchinski. *String theory. Vol. 1: An introduction to the bosonic string*. Cambridge Monographs on Mathematical Physics. Cambridge University Press, Dec. 2007. DOI: [10.1017/CBO9780511816079](https://doi.org/10.1017/CBO9780511816079).
- [12] Ryan A. Rossi and Nesreen K. Ahmed. “The Network Data Repository with Interactive Graph Analytics and Visualization”. In: AAAI. 2015. URL: <https://networkrepository.com>.
- [13] Loring W. Tu. *An Introduction to Manifolds*. Second Edition. Springer, 2011. DOI: [10.1007/978-1-4419-7400-6](https://doi.org/10.1007/978-1-4419-7400-6).
- [14] Timo Weigand. “Introduction to String Theory”. Lecture Notes. 2012.

- [15] Wayne W. Zachary. "An Information Flow Model for Conflict and Fission in Small Groups". In: *The University of Chicago Press Journals* (1997). URL: <https://doi.org/10.1086/jar.33.4.3629752>.